*eng*

MDPI

*Article*

# The Influences of Microwave Irradiation and Heat Treatment on the Dynamic Tensile Response of Granite

**Shu Wang [1,*], Lei Bao [2,3,*], Pujing Yao [1], Jingxuan Xi [1], Ting Zhang [4], Yueqing Guo [4], Xinshuang Wu [1] and Yitong Sun [1]**

[1] PowerChina Northwest Engineering Corporation Limited, Xi'an 710065, China; 19991266191@163.com (P.Y.); 15929991426@163.com (J.X.); wxs19980902@163.com (X.W.); syt13060355886@163.com (Y.S.)
[2] School of Architectural Engineering, Tianjin University, Tianjin 300350, China
[3] Key Laboratory of Earthquake Engineering Simulation and Seismic Resilience of China Earthquake Administration, Tianjin University, Tianjin 300350, China
[4] School of Civil Engineering and Architecture, Xi'an University of Technology, Xi'an 710048, China; z15027316929@163.com (T.Z.); 1870566520gg@gmail.com (Y.G.)
* Correspondence: 13102213129@163.com (S.W.); lbao@tju.edu.cn (L.B.); Tel.: +86-131-0221-3129 (S.W.)

**Abstract:** The paramount significance of temperature's influence on rock engineering endeavors underscores its profound capacity to alter the physical and mechanical attributes of rocks. Among the most crucial techniques utilized to thermally induce damage and diminish the tensile resilience of rock materials are microwave irradiation and heat treatment. This research examines and compares the effects of these two modalities on the dynamic tensile characteristics of Fangshan granite (FG), including their implications under conditions of overload and dependencies on loading rate, utilizing the sophisticated Split Hopkinson Pressure Bar (SHPB) apparatus. In particular, the dynamic real tensile strength (RST) of Brazilian disc (BD) specimens was meticulously gauged and contrasted after subjecting them to microwave irradiation at a potent 6 kW for varying durations (1.5, 3.0, and 4.5 min) and heat treatment across distinct temperature thresholds (178 °C, 345 °C, and 473 °C). To enhance the precision of the measurements, an overload correction was implemented by affixing a strain gauge in close proximity to the core of the BD specimen. The conventional dynamic tensile strength exhibited a reduction of approximately 20 to 30% with the prolongation of microwave radiation time. Furthermore, an additional decrease in tensile strength was observed with the elevation of heat treatment temperatures, reaching a maximum reduction of up to 40%. This phenomenon can be attributed to the proliferation and expansion of microcracks within the rock matrix. It was noteworthy that the RTS, corrected for overloading effects, exhibited a comparable trend to the dynamic traditional tensile strength (TTS). Both were significantly correlated with the loading rate, with the dynamic tensile strength demonstrating an average decrease of approximately 25% when the loading rate was increased. Interpolation and fitting analyses were employed to investigate the effects of microwave radiation duration, heat treatment temperature, and loading rate on the dynamic tensile strength of FG samples. Furthermore, it was established that the overload ratio increased in conjunction with an increase in microwave radiation duration, heat treatment temperature, and loading rate, reaching a maximum value of 1.5.

**Keywords:** microwave irradiation; heat treatment; split Hopkinson pressure bar; dynamic tensile response; overload correction



Academic Editors: Antonio Gil Bravo and Manoj Khandelwal

Received: 18 October 2024
Revised: 16 December 2024
Accepted: 25 December 2024
Published: 26 December 2024

**Citation:** Wang, S.; Bao, L.; Yao, P.; Xi, J.; Zhang, T.; Guo, Y.; Wu, X.; Sun, Y. The Influences of Microwave Irradiation and Heat Treatment on the Dynamic Tensile Response of Granite. *Eng* **2025**, *6*, 3. https://doi.org/10.3390/eng6010003

## 1. Introduction

Rock fragmentation, particularly in deep rock formations, represented a significant challenge in the fields of rock mechanics and rock engineering [1,2]. A reduction in rock fragmentation efficiency often resulted in a decline in excavation efficiency in underground caverns through conventional blasting and mechanical techniques. In recent decades, a number of assisted rock fracturing methods have been developed and proposed, including water jet [3], resonance-enhanced drilling, thermal-assisted rock breaking [4,5], microwave irradiation, and laser power [6,7]. The objective of these methods was to weaken the rock mass to be excavated by applying external energy. In addition, microwave irradiation and heat treatment have been identified as promising and advanced technologies for hard rock fragmentation in the context of drilling and cutting [8]. This was due to their portability and ease of operation in inducing thermal cracks in the rock mass [9,10]. However, their effects on the physico-mechanical properties of rocks, especially their dynamic properties such as dynamic tensile strength, have yet to be fully elucidated. It was, therefore, imperative to gain a deeper understanding of the dynamic response of rocks subjected to microwave irradiation and heat treatment in order to enhance the efficiency of rock fragmentation and facilitate the wider application of these methods.

The thermal instability of minerals renders rocks susceptible to alterations in temperature, which in turn give rise to modifications in the macroscopic mechanical properties of the rock, often manifested as thermally induced microcracks [11–15]. The microwave irradiation method employs energy to induce molecular motion and friction within an object [10,16]. The efficacy of microwave irradiation for heating was contingent upon the intrinsic properties of the material in question, including its transparency, conductivity, and capacity to absorb energy. Nevertheless, only materials with the capacity to absorb microwave radiation were capable of undergoing rapid heating in a relatively short duration of microwave irradiation [7,17]. Among the various constituent minerals of rocks, sulfide, oxide, and iron minerals were optimal absorbers, whereas quartz and feldspar were transparent [18]. Furthermore, the discrepancy in microwave absorptivity among the minerals that constitute rocks can result in thermal damage and uneven deformation of rock specimens. The damage mechanisms for different rock types have been extensively studied due to the considerable variation in mineral constituents [19–21]. Furthermore, the duration and power of microwave irradiation have been found to exert a considerable influence on the quasi-static responses [19]. Furthermore, the drop weight test and the SHPB test were employed to examine the dynamic capacity and fragmentation of microwave-irradiated rocks [21–23]. The impact of the microwave irradiation duration and loading rate on the dynamic uniaxial compressive strength of Fangshan granite was investigated, and the average fragment size of the granite samples treated with microwave irradiation was analyzed [23]. It was demonstrated that microwave irradiation markedly diminished the dynamic tensile properties of granitic rocks [22]. To enhance the efficiency of rock fragmentation, further research is required to gain a deeper understanding of the impact of microcracks introduced by microwaves on rock damage.

The exposure of rocks to high temperatures during heat treatment represented a preconditioning mechanism that resulted in thermal damage, thereby reducing both the static and dynamic mechanical properties of the rocks [24–26]. The heat-treatment method was achieved through the transfer of heat from a high-temperature heat source to a low-temperature object. High-temperature exposure has a profound impact on the mechanical behavior and microstructure of rocks, leading to changes in mineral composition and microstructure, such as the formation of thermal cracks and increased porosity, as well as reductions in quasi-static properties like tensile strength, P-wave velocity, density, and CT value [23,25,27–30]. The dynamic properties of rocks subjected to heat treatment have

been extensively studied using SHPB tests, and it was generally accepted that the dynamic tensile strength of heated rocks was dependent on the loading rate and decreases with increasing temperature at a similar loading rate [15,25]. A conventional SHPB apparatus has been modified with an oven to provide real-time high temperature to the tested rock specimens, and the results demonstrated that the peak stress of heated specimens decreases with increasing temperature [31]. Furthermore, the authors employed the dynamic ball compression test to investigate the fragmentation characteristics of rocks [29]. Their findings indicated that the dynamic tensile strength increases with the loading rate and decreases with the increase in the treatment temperature. Nevertheless, a comprehensive evaluation of the impact of microwave irradiation and heat treatment on the dynamic tensile strength of rocks has yet to be conducted despite the prevalence of external dynamic disturbances, such as explosions and earthquakes, in engineering rock masses.

In this study, dynamic Brazilian disc (BD) tests were conducted on Fangshan granite (FG) specimens that had undergone microwave irradiation and heat treatment using the SHPB apparatus. Furthermore, an overload correction was conducted by affixing a strain gauge in close proximity to the center of the BD specimen. Additionally, the impact of the overload, which can lead to an overestimation of tensile strength due to calculations based on the peak point of the strain curve rather than the fracture onset, has been taken into account and corrected in the strength data. Subsequently, the impact of microwave irradiation and heat treatment on the FG specimens was investigated with regard to the overload ratio. Three comparison groups were conducted to ascertain the impact of microwave irradiation and heat treatment on the dynamic tensile strength.

The objective of this study was to gain insight into the effects of microwave radiation and thermal treatments on the dynamic tensile strength of granite, with the aim of addressing scientific questions in the field of rock engineering regarding the effectiveness of non-traditional rock crushing techniques. The study involved experiments with microwave radiation and heat treatments at varying temperatures on Fangshan granite (FG) samples to assess the impact of these treatments on the physical and mechanical properties of the rock. By conducting dynamic Brazilian disc (BD) tests with a cutting-edge SHPB apparatus, we were able to quantify the impact of microwave radiation duration and heat treatment temperature on the dynamic tensile strength of granite. The findings demonstrated the microscopic crack expansion and proliferation in the rock resulting from microwave radiation and heat treatment and how these changes markedly diminish the rock's dynamic tensile strength. Furthermore, the study examined the impact of overload correction on dynamic tensile strength measurements and investigated the combined influence of microwave radiation duration, heat treatment temperature, and loading rate on the dynamic tensile strength of granite through interpolation and fitting analysis. These findings have significant implications for engineering practice, particularly in the context of improving rock crushing efficiency and optimizing mining engineering procedures.

## 2. Materials and Methods

### *2.1. Specimen Preparation*

It has been observed that granite, a material commonly encountered in tunneling excavation projects, exhibits sensitivity to microwave irradiation [32]. In this study, the specimen was selected as Fangshan granite (FG) from Beijing. A compositional analysis was conducted to ascertain its suitability for microwave exposure. X-ray diffraction analysis revealed that the FG specimen comprised 59.4% albite, calcian-ordered, 33.6% quartz, 4% annite, and 3% greenalite [23]. Annite and greenalite were classified as distinct mineralogical species. Annite was a member of the biotite mica group, while greenalite was a member of the serpentine group. The minerals in question possess notable microwave-

absorbing properties as a consequence of their chemical composition, which included the presence of iron (Fe). The presence of iron (Fe) in their chemical composition enhances their ability to absorb microwaves in comparison to albite and quartz, which lack significant amounts of Fe [33]. In this study, a Brazilian disc (BD) test was conducted using a disc with a diameter of 50 mm and a thickness of 25 mm.

Prior to microwave irradiation of FG specimens, a preconditioning process was conducted using a CM-06S multimode cavity microwave system operating at a frequency of 2.45 GHz and a power of 6 kW. To prevent the occurrence of cracking due to moisture absorption, the specimens were subjected to a drying process in an electric furnace at a temperature of 105 °C for a period of 24 h prior to undergoing microwave treatment. A visual observation of the main crack and the local melt zone was conducted after 5.0 min of irradiation, indicating that the microwave irradiation duration should not exceed 5 min. To further examine the influence of microwave exposure duration on the specimens, the irradiation was conducted for distinct durations of 0 min, 1.5 min, 3 min, and 4.5 min.

In order to compare the effect of microwave irradiation and heat treatment on the dynamic tensile strength of FG, it was necessary to use the static tensile strength of microwave-irradiated FG as a reference index. The initial testing was conducted using heat-treatment temperatures of 150 °C, 250 °C, 500 °C, and 750 °C. The outcomes of the static tensile strength assessments conducted on FG following heat treatment and microwave irradiation are illustrated in Figure 1. Upon completion of the heat-treatment process, the furnace was deactivated and allowed to return to ambient temperature. Figure 1 illustrates the alterations in the static tensile strength of Fangshan granite subsequent to microwave radiation and heat treatment at varying temperatures. Following preliminary fitting calculations and supplementary testing, the corresponding microwave irradiation durations and heat-treatment temperatures for the comparison groups were identified as 0 min and 25 degrees Celsius, 1.5 min and 178 degrees Celsius, 3 min and 345 degrees Celsius, and 4.5 min and 473 degrees Celsius, respectively. Additionally, a reference group of BD specimens that had not undergone microwave irradiation or heat treatment was prepared.

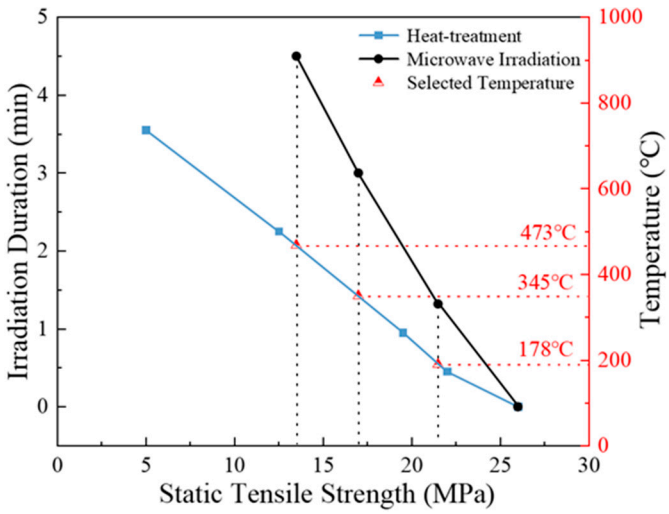


**Figure 1.** Comparison of static tensile strength of FG damaged by microwave irradiation and heat treatment.

To assess the impact of heat treatment on the dynamic tensile strength of FG, experiments were conducted in a servo-controlled electric furnace. The specimens were heated at a gradual rate of 2 °C/min to prevent the occurrence of thermal shock cracking. This slow heating rate was selected to minimize the potential for thermal stress [8]. Upon completion of the heat-treatment process, the furnace was deactivated and allowed to return to ambient

temperature. The application of microwave radiation to the rock resulted in the generation of heat, which in turn excited molecular vibration and friction. This process led to the expansion of existing microcracks and the formation of new cracks. In contrast, heat treatment has been observed to increase the porosity of the rock through cycles of thermal expansion and contraction, potentially accompanied by mineral phase changes. This phenomenon has been linked to a reduction in the rock's static tensile strength. These changes reflected damage to the microstructure and degradation of the macroscopic mechanical properties of the rock and were essential for understanding and predicting the behavior of rocks in engineering applications.

### *2.2. Specimen Characterization*

In order to quantify the thermal damage sustained by the microwave-irradiated and heat-treated FG specimens, an X-ray computerized tomography (CT) method was employed in this study. Prior research has established the efficacy of CT in quantifying damage to rocks resulting from microwave irradiation and heat treatment [27,34], and the CT value $H_{rm}$ can be defined as follows:

$$H_{rm} = \frac{\mu_r^m - \mu_w^m}{\mu_w^m} \times 1000 \quad (1)$$

where $\mu_r^m$ and $\mu_w^m$ are mass absorbing coefficients for rock and water.

Another common method for assessing rock damage was the use of ultrasonic techniques to determine the P-wave velocities [35]. In this study, the technique was also utilized to quantify the P-wave velocities of specimens that had been subjected to microwave irradiation and heat treatment.

The results of these measurements were presented in Tables 1 and 2, which demonstrated the variations in P-wave velocities and CT values for the damaged FG specimens. The results demonstrated a decline in both P-wave velocity and CT value as the duration of irradiation and temperature of heat-treatment increase. In the case of microwave irradiation, the FG specimens listed in Table 1 exhibited a relatively rapid decrease in P-wave velocity and CT value during the initial 2 min of exposure. However, during the 2–4.5 min interval, the decrease in P-wave velocity and CT value was relatively gradual. The P-wave velocity exhibited a rapid decline, reaching 3524 m/s within two minutes, which represented an 80.5% reduction compared to the unirradiated specimen. Subsequently, the P-wave velocity exhibited a gradual decline, reaching 2927 m/s at 4.5 min, which represents a 66.9% reduction compared to the velocity observed in the unirradiated specimen. The declining trend of CT values exhibited a comparable pattern, with a pronounced decline to 1729 $H_u$ at the two-minute mark, representing approximately 75.3% of the unirradiated specimen. It was followed by a gradual decline to 1602 $H_u$ at the four-and-a-half-minute mark, which equates to approximately 69.7% of the initial value. The observed decline in P-wave velocity and CT value can be attributed to the proliferation of microcracks within the specimen as a consequence of irradiation [36]. The reduction in P-wave velocity and CT value of the heat-treated FG specimen displayed a notable divergence from that of the microwave-irradiated FG specimen. As illustrated in Table 2, there was a precipitous decline in both P-wave velocity and CT values as the temperature increased from room temperature up to 600 °C. However, the rate of decrease was comparatively gradual when the temperature ranged from 600 to 800 °C. The notable decline in P-wave velocity and CT values within the temperature span of 25 to 600 °C can be ascribed to the expansion of fissures caused by thermal stresses and the transformation of quartz from α to β at 573 °C [25]. In the present study, the maximum temperature employed for the heat treatment was 473 °C.

**Table 1.** Variation of P-wave velocities and CT values of microwave-irradiation-damaged FG.

| Irradiation Duration (min) | P-Wave (m/s) | CT-Value ($H_u$) |
|---|---|---|
| 0 | 4375 | 2297 |
| 1.5 | 3686 | 2184 |
| 2.0 | 3524 | 1729 |
| 2.5 | 3483 | 1698 |
| 3.0 | 3394 | 1693 |
| 3.5 | 3297 | 1686 |
| 4.0 | 3105 | 1657 |
| 4.5 | 2927 | 1602 |

**Table 2.** Variation of P-wave velocities and CT values of heat-treatment-damaged FG.

| Irradiation Duration (min) | P-Wave (m/s) | CT-Value ($H_u$) |
|---|---|---|
| 25 | 4428 | 2284 |
| 178 | 4273 | 2207 |
| 223 | 4159 | 2117 |
| 345 | 3628 | 1905 |
| 473 | 1824 | 1796 |
| 600 | 1564 | 1733 |
| 800 | 977 | 1709 |

### *2.3. Split Hopkinson Pressure Bar (SHPB) System*

In accordance with the ISRM recommended methods for determining dynamic rock tensile strength [37], the dynamic tensile strength was measured using an SHPB system. The system consisted of a striker bar, an incident bar with a length of 3000 mm, and a transmitted bar of 1800 mm length, all of which had identical diameters of 50 mm (as illustrated in Figure 2).

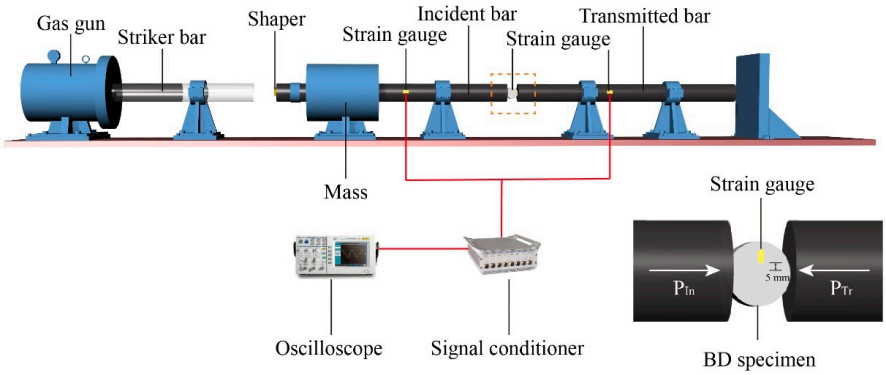


**Figure 2.** Schematic of the Split Hopkinson Pressure Bar system.

The BD specimen was initially positioned between the incident bar and the transmitted bar and subsequently struck by the striker at the free end of the incident bar. This results in the generation of an incident wave, designated as $\varepsilon_i$, within the incident bar. The interaction between the incident wave and the specimen gives rise to the formation of two supplementary waves: the reflected wave, denoted as $\varepsilon_r$, and the transmitted wave, denoted as $\varepsilon_t$ (Figure 3). By analyzing the measured strains of these three waves, it was possible to calculate the normal forces acting on both ends of the specimen:

$$P_{In} = AE(\varepsilon_i + \varepsilon_r) \quad (2)$$

$$P_{Tr} = AE\varepsilon_t \quad (3)$$

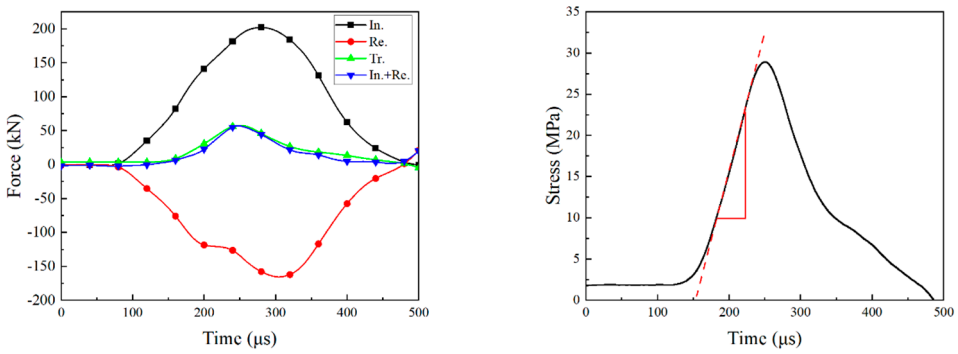


**Figure 3.** Dynamic force balance and determination of loading rate for a typical dynamic test (the symbols In., Re., and Tr. are referred to as incident, reflected, and transmitted, respectively).

In this context, the dynamic forces acting on the incident and transmitted ends were represented by the symbol "$P_{In}$, $P_{Tr}$". The symbol "$A$" represented the cross-sectional area of the bars, the symbol "$E = 211$ GPa" represented the Young's modulus of the bars, and the symbols "$\varepsilon_i$", "$\varepsilon_r$", and "$\varepsilon_t$" represented the strain signals corresponding to the incident, reflected, and transmitted waves, respectively. In the case of rock material subjected to dynamic loading, the pulse shaper has been introduced as a means of eliminating the inertia effect [37]. In the present study, copper shapers with a diameter of 9 mm and a thickness of 0.9 mm were employed for each test.

The tensile stress in the central disc along the loading direction can be calculated using the following equation [37]:

$$\sigma_{(t)} = \frac{2P(t)}{\pi BD} \tag{4}$$

where $P(t)$ was the loading force, and $B$ and $D$ were the thickness and diameter of the BD specimen, respectively. Tensile strength $\sigma$ was determined as the maximum value of $\sigma_{(t)}$. It has been noted that the validation of using the static stress analysis Equation (4) for dynamic data reduction was that dynamic force balance was achieved across the BD specimen during dynamic testing [37,38].

In order to evaluate the dynamic balance, it was necessary to calculate two dynamic forces, which can be achieved through the use of Equations (2) and (3). A typical dynamic test, as illustrated in Figure 3, was conducted to demonstrate the similarity of the load period dynamics, effectively eliminating the effect of inertia. Consequently, the equilibrium of dynamic forces on both ends of the specimen was established. It was determined that Equation (4), which was originally derived under the assumption of static loading, remains valid for dynamic loading conditions provided that the dynamic forces are in equilibrium. Moreover, the loading rate can be defined by examining the temporal variation of local tensile stress. This can be achieved by analyzing the slope of the linear portion of the tensile stress curve that occurs prior to the peak stress, as illustrated in Figure 3.

### *2.4. Correction for Dynamic BD Tensile Strength*

The indirect measurement of tensile strength in the BD test has been demonstrated in several studies to potentially overestimate the tensile strength of rock samples due to the occurrence of overload [39–42]. Accordingly, the result yielded by Equation (4) represented the conventional tensile stress (TTS), which can be adjusted to obtain the RTS [40,43]. To accurately determine the central cracking moment during dynamic loading, a strain gauge was placed at a distance of 5 mm from the center of the specimen to monitor the onset of fracture, as illustrated in Figure 2.

As illustrated in Figure 4, the turning point B in the recorded strain signal was a consequence of the elastic dissipation wave generated at the onset of crack propagation. By subtracting the propagation time from the moment of turning point B, the precise time of primary crack initiation can be determined, and the tensile stress (point C) at that time can be accurately determined [22]. As a result, the TTS (the tensile stress at point A) can be corrected to obtain the RTS (the tensile stress at point C) [41]. It was also important to note that the overload ratio was not constant and that the overload effect was subjected to careful evaluation for each test.

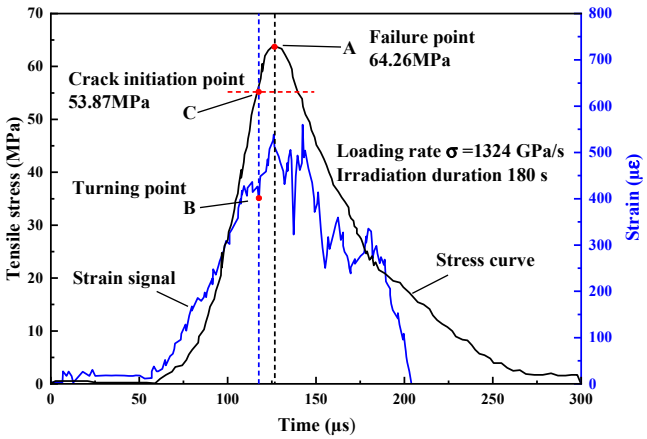


**Figure 4.** A typical dynamic BD test for demonstrating the overload effect.

Figure 4 illustrates the alterations in the internal microstructure of the granite following microwave radiation and heat treatment, which directly influence the macroscopic mechanical properties of the rock. The microanalysis results demonstrated that microwave radiation and heat treatment induced the expansion of existing microcracks and the formation of new cracks, resulting in a reduction in the dynamic tensile strength of the rock. The data in Figure 4, corrected for overloading, provide a more accurate representation of the dynamic RTS, which was a more precise reflection of the mechanical behavior of the rock material than the uncorrected conventional dynamic TTS. This finding has significant engineering applications, including the optimization of rock-crushing technology, the enhancement of mining engineering efficiency, and the guidance of rock-engineering practice. Additionally, it offers new insights for scientific research in the field of rock mechanics.

## 3. Results and Discussion

### *3.1. Effects of Microwave Irradiation and Heat Treatment on Tensile Strength*

In the dynamic BD test, the cracks develop from the geometric center and split along the compressive diametric line [15,44]. Figure 5 illustrates the typical tensile failure modes observed in FG specimens subjected to microwave irradiation and heat treatment. Under comparable loading rates, the BD specimens that had not undergone microwave irradiation and heat treatment exhibited failure in the direction of loading, with the fracture surface displaying two semicircular patterns. It was noteworthy that the FG specimens that underwent heat treatment exhibited greater damage than the microwave irradiation specimens within the same group. This observation can be attributed to the presence of a greater number of transgranular cracks in the quartz within the heat-treatment specimens, which resulted in a reduction in dynamic tensile strength and ultimately led to a more severe level of damage to the specimens [45].

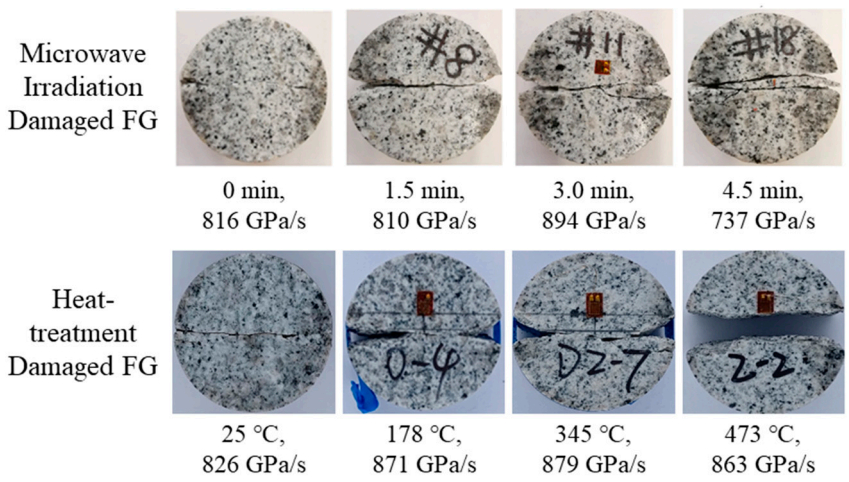


**Figure 5.** Typical tensile failure modes of microwave-irradiation and heat-treatment-damaged FG.

Figure 6 illustrates the dynamic TTS and RTS of FG specimens that have been damaged by microwave irradiation and heat treatment. The findings of the study demonstrated a consistent elevation in the TTS and RTS values of the FG specimens as the loading rate increases. Furthermore, a dependence of these values on the loading rate was also observed. When the loading rates were comparable, a significant decrease in both TTS and RTS was observed as both the duration of microwave irradiation and the temperature of the heat treatment were increased.

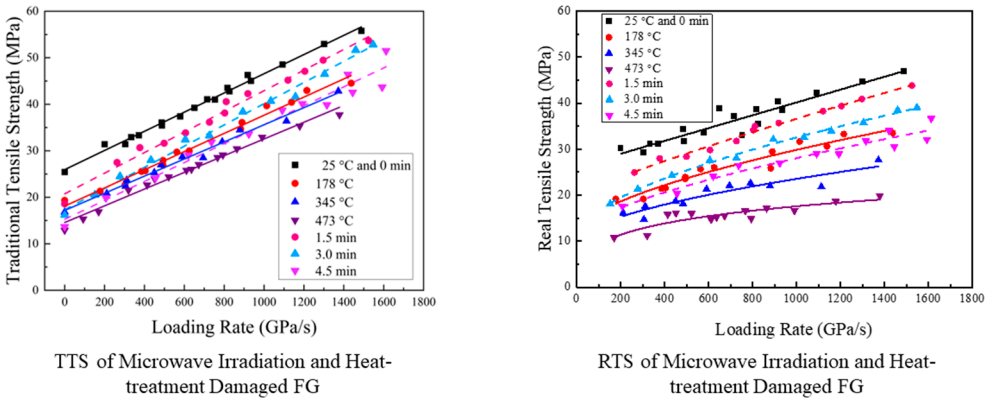


**Figure 6.** TTS and RTS of microwave-irradiation and heat-treatment-damaged FG.

A linear fitting method was selected for the purpose of fitting the TTS of FG under a variety of microwave irradiation durations and heat-treatment conditions, as described by Equations (5) and (6).

Various microwave irradiation durations:

$$\sigma_{tm} = a_m \frac{\dot{\sigma}}{\dot{\sigma}_0} + \sigma_{tm0} \tag{5}$$

Various heat-treatment temperatures:

$$\sigma_{th} = a_h \frac{\dot{\sigma}}{\dot{\sigma}_0} + \sigma_{th0} \tag{6}$$

where $\sigma_{tm}$ and $\sigma_{th}$ were the TTS of microwave-irradiation and heat-treatment-damaged FG specimen, $a_m$, $a_h$, $\sigma_{tm0}$, and $\sigma_{th0}$ were fitting parameters, and $\dot{\sigma}_0$ and $\dot{\sigma}$ were quasi static and dynamic loading rates. The results of the fitting procedures were presented in Tables 3 and 4, respectively.

**Table 3.** Fitting parameters of TTS of microwave irradiation FG specimen.

| Durations/Min | Fitting Parameters | | $R^2$ |
|---|---|---|---|
| | $a_m$ | $\sigma_{tm0}$ | |
| 0 | $2.06 \times 10^{-5}$ | 25.95 | 0.99 |
| 1.5 | $2.22 \times 10^{-5}$ | 20.74 | 0.99 |
| 3.0 | $2.28 \times 10^{-5}$ | 17.32 | 0.99 |
| 4.5 | $2.03 \times 10^{-5}$ | 15.26 | 0.96 |

**Table 4.** Fitting parameters of TTS of heat-treatment FG specimen.

| Temperatures/°C | Fitting Parameters | | $R^2$ |
|---|---|---|---|
| | $a_h$ | $\sigma_{th0}$ | |
| 25 | $2.0613 \times 10^{-5}$ | 25.9450 | 0.99 |
| 178 | $1.9532 \times 10^{-5}$ | 18.1058 | 0.98 |
| 345 | $1.8417 \times 10^{-5}$ | 17.1836 | 0.99 |
| 473 | $1.7695 \times 10^{-5}$ | 14.8166 | 0.96 |

The loading rate for the TTS of FG specimens from microwave irradiation and heat-treatment exhibited an initial increasing trend, followed by a subsequent decrease. The maximum values were attained at a duration of 3.0 min for microwave irradiation and a temperature of 345 °C for heat treatment, respectively.

Following correction, the RTS values of the FG specimens were found to exhibit a non-linear relationship with the loading rate. The rate of increase in RTS was observed to decline as the loading rate increased. Consequently, Equations (7) and (8) were selected for fitting in order to more accurately represent this relationship.

Various microwave irradiation durations:

$$\sigma_{rm} = a_m + b_m \dot{\sigma}^{c_m} \tag{7}$$

Various heat-treatment temperatures:

$$\sigma_{rh} = a_h + b_h \dot{\sigma}^{c_h} \tag{8}$$

where $\sigma_{rm}$ and $\sigma_{rh}$ were the RTS of microwave irradiation and heat-treatment FG specimen, $\dot{\sigma}$ was dynamic loading rates, and $a_m$, $a_h$, $b_m$, $b_h$, $c_m$, and $c_h$ were fitting parameters. The results of the fitting were presented in Tables 5 and 6, respectively.

**Table 5.** Fitting parameters of RTS of microwave irradiation FG specimen.

| Durations/Min | Fitting Parameters | | | $R^2$ |
|---|---|---|---|---|
| | $a_m$ | $b_m$ | $c_m$ | |
| 1.5 | 19.5241 | 0.0501 | 0.8442 | 0.94 |
| 3.0 | 11.5600 | 0.3212 | 0.6050 | 0.94 |
| 4.5 | 11.6728 | 0.1664 | 0.6644 | 0.93 |

As illustrated in Figure 7, the data fitting and interpolation calculations revealed significant discrepancies between TTS and RTS in response to diverse thermal treatment modalities.

**Table 6.** Fitting parameters of RTS of heat-treatment FG specimen.

| Temperatures/°C | Fitting Parameters | | | $R^2$ |
|---|---|---|---|---|
| | $a_h$ | $b_h$ | $c_h$ | |
| 178 | 12.0251 | 0.2533 | 0.6158 | 0.95 |
| 345 | 9.6946 | 0.2827 | 0.5633 | 0.93 |
| 473 | 9.7713 | 9.0758 | 0.1597 | 0.93 |

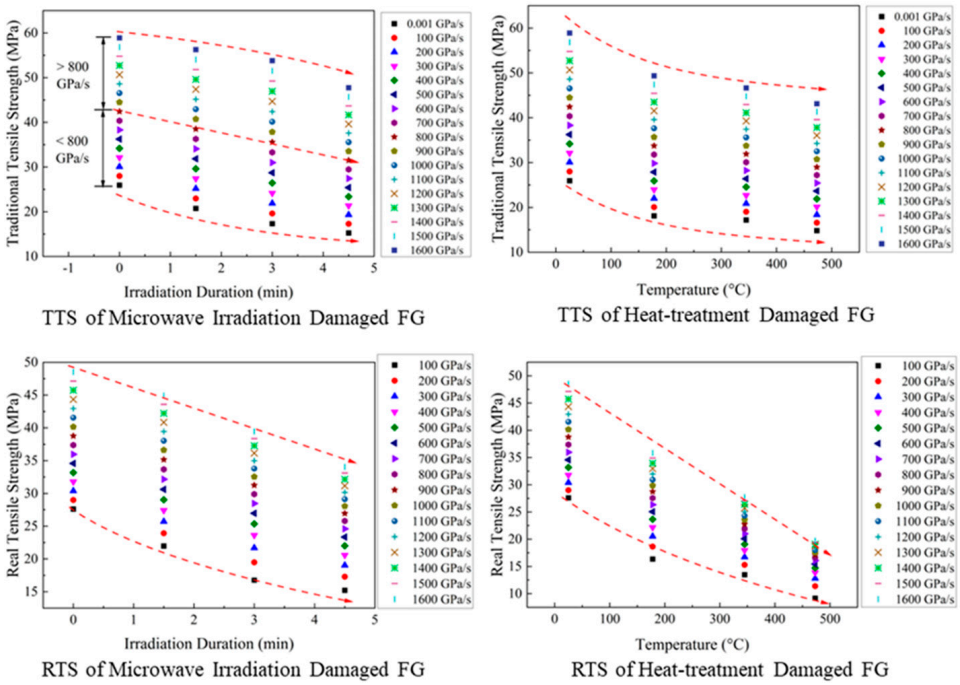


**Figure 7.** The disparities between TTS and RTS under various treatment methods.

In the case of microwave-irradiation-induced damage to FG, the dynamic TTS was observed to decrease as the duration of microwave irradiation damage increased. Furthermore, the rate of this decrease was also influenced by the loading rate. When the loading rate was below 800 GPa/s, the rate of decrease in TTS was observed to decrease with increasing irradiation duration. However, when the loading rate exceeded 800 GPa/s, the TTS decrease rate increased with the duration. At a loading rate approaching 800 GPa/s, the TTS was nearly proportional to the duration. Furthermore, the RTS obtained through correction was linear with respect to the irradiation duration for high loading rates, whereas it decreased at a slower rate with increasing duration at low loading rates.

In the case of heat-treated FG, the TTS initially decreased at a rapid rate and then decelerated as the temperature rose. This suggests that the detrimental impact of temperature on the TTS diminishes with declining temperature at a consistent loading rate. Moreover, the TTS curves displayed a parallel pattern at varying loading rates, indicating that the loading rate exerts a negligible influence on the TTS variation with temperature. Additionally, the RTS demonstrated a decline as temperature increases. Moreover, a higher loading rate resulted in a closer relationship between the RTS and temperature, which approached a linear correlation.

The generation of contour clouds through interpolation and fitting calculations offers valuable insight into the interplay between dynamic tensile strength and its strengthening and weakening effects. Specifically, it allowed for the examination of how increased loading rates and microwave irradiation duration and heat-treatment temperature affect the tensile strength of a material.

The aforementioned calculations provided a comprehensive evaluation of the impact of these factors on the dynamic tensile strength of the specimen (Figure 8). The TTS contour cloud of microwave irradiation FG indicated that the TTS was influenced by the interaction between the loading rate and the duration of microwave irradiation. The intensity profile exhibited a variation pattern comprising two distinct areas. In Area I, an increase in the loading rate resulted in a corresponding increase in the strengthening effect of the loading rate, while the weakening effect of temperature was observed to decrease. In contrast, in Area II, the strengthening effect of the loading rate was observed to diminish, while the weakening effect of temperature was seen to intensify as the loading rate rises.

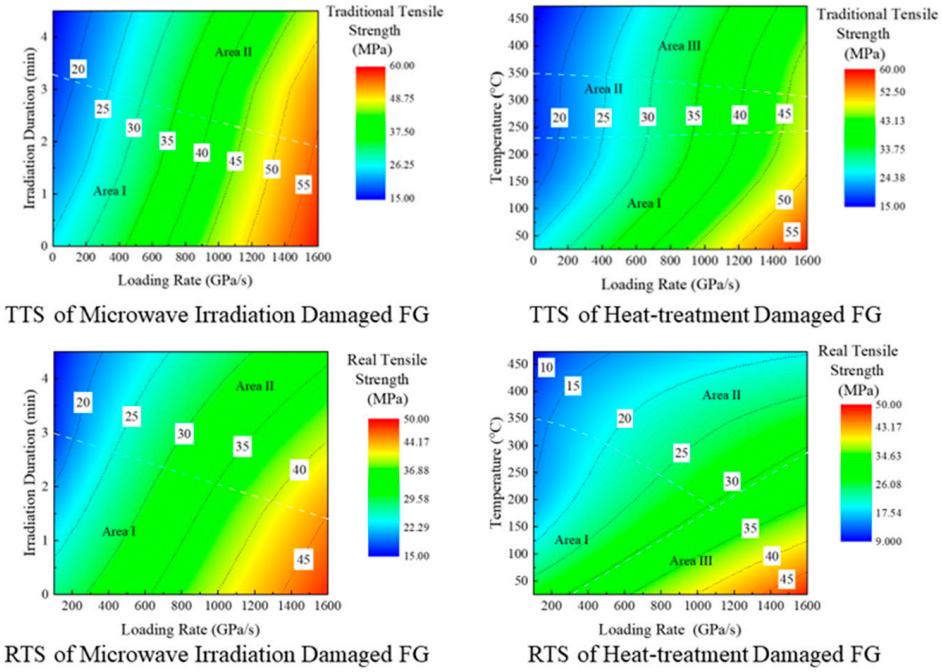


**Figure 8.** Contour clouds of microwave-irradiated and heat-treatment FG TTS and RTS: TTS of microwave-irradiation-damaged FG; TTS of heat-treatment-damaged FG; RTS of microwave-irradiation-damaged FG; RTS of heat-treatment-damaged FG.

The contour cloud of the RTS of microwave-irradiation-damaged FG also exhibited notable variations. In Area I, the strengthening effect of the loading rate and the weakening effect of temperature remain relatively constant as the loading rate increases. In contrast, in Area II, the strengthening effect of the loading rate was observed to diminish, while the weakening effect of microwave irradiation was seen to increase.

The contour cloud of the TTS of heat-treatment-damaged FG can be divided into three distinct areas. In Area I, the strengthening effect of the loading rate increases, while the weakening effect of temperature decreased, with an increasing loading rate. In Area II, the predominant factor influencing TTS was the loading rate, with temperature fluctuations having a minimal impact. The TTS remained primarily influenced by the strengthening effect of the loading rate, regardless of any variations in temperature. In Area III, a decline in the strengthening effect of the loading rate was observed, while an increase in temperature led to a corresponding increase in the weakening effect. Consequently, the TTS was primarily affected by the temperature change, with the loading rate having a secondary effect.

The results of the RTS contour clouds analysis of heat-treatment-damaged FG demonstrate notable variations in the loading rate strengthening effect and temperature weakening effect across three discrete areas. In Area I, a positive correlation was observed between the loading rate strengthening effect and the increasing loading rate. Conversely, the

temperature weakening effect demonstrated a decrease with increasing loading rate. In contrast, in Area II, the strengthening effect of the loading rate was observed to decrease with increasing loading rate, while the temperature weakening effect was seen to increase. In Area III, however, the influence of these two effects was found to be relatively stable.

### *3.2. Effects of Microwave Irradiation and Heat Treatment on Overload Ratio*

The dynamic BD test, as an indirect method for determining tensile strength, may overestimate the dynamic tensile strength of the rocks; therefore, the overload ratio can be introduced as a metric to estimate the overload phenomenon [46]. The overload ratio was defined as the proportion of the difference between the TTS and RTS, expressed as a percentage of the TTS. Figure 9 illustrates the variation in the overload ratio observed in the dynamic BD test at varying microwave irradiation durations and heat-treatment temperatures.

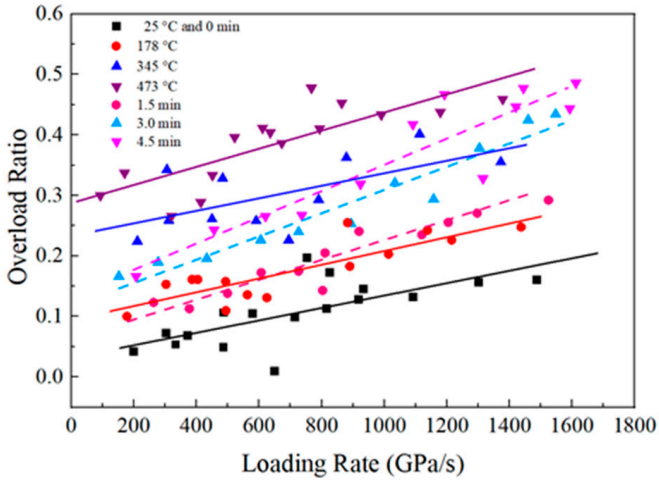


**Figure 9.** The overload ratio in dynamic BD test under various microwave irradiation durations and heat-treatment temperatures.

The study revealed that the overload ratio of FG exhibited an increase with the prolongation of microwave irradiation and the elevation of heat-treatment temperature. A correlation between the overload ratio and the loading rate has been identified. The overload ratios of heat-treated FG specimens exhibit higher values than those of microwave-irradiated FG specimens. At temperatures reaching 473 °C or microwave irradiation durations of 4.5 min, overload ratios exceeding 0.4 can be observed under high loading conditions. This observation indicated that the calculated dynamic tensile strength of the FG specimen that has undergone thermal modification through microwave irradiation and heat treatment was significantly overestimated when the TTS was employed as a universal index for determining dynamic tensile strength.

### *3.3. Effects Degree of Microwave Irradiation and Heat Treatment in Comparison Group*

The present study investigated the dynamic tensile mechanical behavior of FG subjected to different thermal modification techniques through experimental analysis. Figure 10 presents the TTS and RTS of FG after various thermal modification methods in comparison groups. The solid lines represent the fitted curves of heat-treated FG, while the dashed lines represent the fitted curves of microwave-irradiated FG.

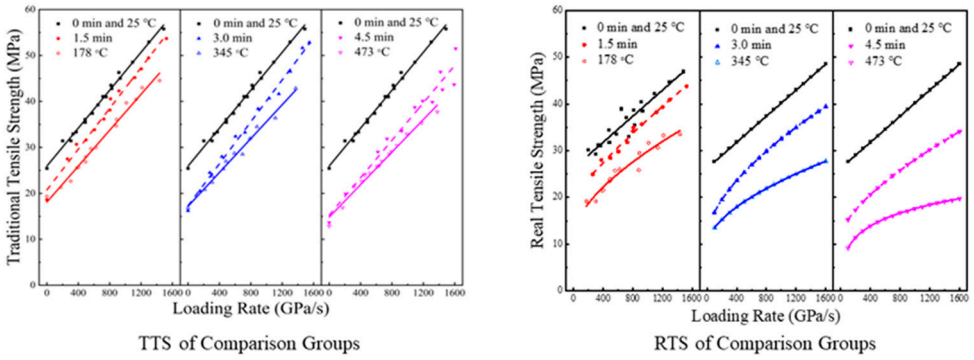


**Figure 10.** TTS and RTS of the comparison groups.

The findings demonstrated that the tensile strength of heat-treated FG was inferior to that of microwave-treated FG within the same comparison group. In the context of dynamic tensile loading, it has been observed that FG specimens subjected to microwave irradiation demonstrate an elevated propensity for cracking in the direction of pre-existing microcracks [45]. Moreover, the reduced prevalence of transgranular cracks in quartz within the microwave irradiation FG specimens, when compared to the heat-treatment FG specimens, leads to an enhanced dynamic tensile strength of the former. Additionally, the strength of quartz in granite minerals was relatively high, contributing significantly to the overall strength of the rock [46]. However, the heat treatment of FG specimens resulted in a more uniform distribution of internal cracks, which increased the number of microcracks in quartz and consequently led to a lower dynamic tensile strength compared to microwave irradiation specimens.

## 4. Conclusions

The objective of this study was to investigate the impact of microwave irradiation and heat treatment on the dynamic tensile responses of FG specimens. To this end, dynamic Brazilian disc (BD) tests were performed using the SHPB apparatus on both microwave irradiation and heat-treatment FG specimens. The study took into account the potential for an overload effect, whereby tensile strength may be overestimated due to the calculation of strength at the peak point of the strain curve, rather than at the point of fracture initiation. The results were obtained through three comparison groups, with the objective of determining the differences between the effects of microwave irradiation and heat treatment on the dynamic tensile strength of FG.

(1) The TTS and RTS of the FG specimens demonstrated a pronounced correlation with the loading rate. When subjected to comparable loading rate conditions, the TTS of the heat-treated FG was observed to be lower than that of the microwave-irradiated FG. Moreover, the TTS demonstrated a negative correlation with both the duration of microwave irradiation and the heat-treatment temperature. Furthermore, the BD test results were corrected to obtain the RTS. In contrast, the RTS of the heat-treatment FG specimens was observed to be lower than that of the microwave irradiation FG specimens. Additionally, its dependence on the loading rates was noted to be weaker with increasing loading rates. Furthermore, the RTS demonstrated a declining pattern with the extension of microwave irradiation duration and the elevation of heat-treatment temperature.

(2) The dynamic tensile strength of FG specimens was subjected to analysis for both strengthening and weakening effects, employing interpolation and fitting calculations. This study comprehensively considers the effects of microwave irradiation duration, heat-treatment temperature, and loading rate on the dynamic tensile strength. The

findings of this analysis offer significant insight into the influence of these variables on the dynamic tensile strength of FG specimens.

(3) Additionally, the overload ratio was determined to be a function of the loading rate, irradiation duration, and heat-treatment temperature. In the same comparison group, the overload ratios of heat-treatment FG are typically higher than those of microwave irradiation FG. Moreover, the dynamic tensile strength of heat-treated FG is inferior to that of microwave-treated FG within the same comparison group.

Further research could elucidate the mechanical response of diverse rock types to microwave radiation and thermal treatments, as well as the prospective applications of these treatments in various engineering contexts. Furthermore, research could be expanded to encompass the effects of microwave radiation and thermal treatments on additional mechanical properties of rocks, such as the modulus of elasticity and Poisson's ratio, as well as the potential environmental consequences of these treatments.

In light of the findings of this study, it was recommended that microwave radiation and thermal treatments be considered as potential technologies for rock fragmentation and engineering optimization in the design and implementation of rock engineering. Furthermore, it is advised that advanced analytical techniques, such as microanalysis, be employed to evaluate microstructural alterations in rocks, thereby facilitating more precise predictions and control over the mechanical behavior of rocks in pertinent engineering applications. Additionally, dynamic monitoring may be incorporated into rock engineering practices to evaluate the mechanical properties of rocks in real time, thereby ensuring the safety of engineering operations.

**Author Contributions:** Methodology, S.W., X.W. and Y.S.; investigation, S.W. and L.B.; data curation, J.X., T.Z. and Y.G.; writing—original draft preparation, S.W.; writing—review and editing, L.B.; visualization, J.X.; supervision, P.Y.; funding acquisition, L.B. and P.Y. All authors have read and agreed to the published version of the manuscript.

**Funding:** This research was funded by Power China Northwest Engineering Corporation Limited key technology projects (No. XBY-KJ-2024-59), and Tianjin Science and Technology Program (No. 23ZYYYJC00010), and partly supported by the National Natural Science Foundation of China (No. 42307108).

**Institutional Review Board Statement:** Ethical review and approval were waived for this study as it did not involve human or animal research.

**Informed Consent Statement:** Informed consent was obtained from all subjects involved in the study.

**Data Availability Statement:** Data are contained within the article.

**Conflicts of Interest:** Authors Shu Wang, Jingxuan Xi, Xinshuang Wu, Yitong Sun, and Pujing Yao are employed by Power China Northwest Engineering Corporation Limited. The authors declare no conflicts of interest. This research was funded by Power China Northwest Engineering Corporation Limited. The funder was not involved in the study design, collection, analysis, interpretation of data, the writing of this article or the decision to submit it for publication.

## References

1. Bamford, T.; Esmaeili, K.; Schoellig, A.P. A deep learning approach for rock fragmentation analysis. *Int. J. Rock Mech. Min. Sci.* **2021**, *145*, 104839. [CrossRef]
2. Zheng, L.; Zuo, Y.; Hu, Y.; Wu, W. Deformation Mechanism and Support Technology of Deep and High-Stress Soft Rock Roadway. *Adv. Civ. Eng.* **2021**, *2021*, 6634299. [CrossRef]
3. Li, S.; Vaziri, V.; Kapitaniak, M.; Millett, J.M.; Wiercigroch, M. Application of Resonance Enhanced Drilling to coring. *J. Pet. Sci. Eng.* **2020**, *188*, 106866. [CrossRef]
4. Mahanta, B.; Ranjith, P.G.; Vishal, V.; Singh, T.N. Temperature-induced deformational responses and microstructural alteration of sandstone. *J. Pet. Sci. Eng.* **2020**, *192*, 107239. [CrossRef]

5. Deyab, S.M.; Rafezi, H.; Hassani, F.; Kermani, M.; Sasmito, A.P. Experimental investigation on the effects of microwave irradiation on kimberlite and granite rocks. *J. Rock Mech. Geotech. Eng.* **2021**, *13*, 267–274. [CrossRef]
6. Lu, G.; Li, Y.; Hassani, F.; Zhang, X. Review of theoretical and experimental studies on mechanical rock fragmentation using microwave-assisted approach. *Chin. J. Geotech. Eng.* **2016**, *38*, 1497–1506.
7. Lu, G.-m.; Li, Y.-h.; Hassani, F.; Zhang, X. The influence of microwave irradiation on thermal properties of main rock-forming minerals. *Appl. Therm. Eng.* **2017**, *112*, 1523–1532. [CrossRef]
8. Xu, T.; Yuan, Y.; Heap, M.J.; Zhou, G.-L.; Perera, M.S.A.; Ranjith, P.G. Microwave-assisted damage and fracturing of hard rocks and its implications for effective mineral resources recovery. *Miner. Eng.* **2021**, *160*, 106663. [CrossRef]
9. Leroy, M.N.L.; Marius, F.W.; Francois, N. Experimental and Theoretical Investigations of Hard Rocks at High Temperature: Applications in Civil Engineering. *Adv. Civ. Eng.* **2021**, *2021*, 8893944. [CrossRef]
10. Wei, W.; Shao, Z.; Zhang, Y.; Qiao, R.; Gao, J. Fundamentals and applications of microwave energy in rock and concrete processing—A review. *Appl. Therm. Eng.* **2019**, *157*, 113751. [CrossRef]
11. Fan, L.F.; Gao, J.W.; Wu, Z.J.; Yang, S.Q.; Ma, G.W. An investigation of thermal effects on micro-properties of granite by X-ray CT technique. *Appl. Therm. Eng.* **2018**, *140*, 505–519. [CrossRef]
12. Peng, J.; Rong, G.; Yao, M.; Wong, L.N.Y.; Tang, Z. Acoustic emission characteristics of a fine-grained marble with different thermal damages and specimen sizes. *Bull. Eng. Geol. Environ.* **2019**, *78*, 4479–4491. [CrossRef]
13. Rong, G.; Peng, J.; Cai, M.; Yao, M.; Zhou, C.; Sha, S. Experimental investigation of thermal cycling effect on physical and mechanical properties of bedrocks in geothermal fields. *Appl. Therm. Eng.* **2018**, *141*, 174–185. [CrossRef]
14. Tian, W.-L.; Yang, S.-Q.; Elsworth, D.; Wang, J.-G.; Li, X.-Z. Permeability evolution and crack characteristics in granite under treatment at high temperature. *Int. J. Rock Mech. Min. Sci.* **2020**, *134*, 104461. [CrossRef]
15. Yin, T.; Li, X.; Cao, W.; Xia, K. Effects of Thermal Treatment on Tensile Strength of Laurentian Granite Using Brazilian Test. *Rock Mech. Rock Eng.* **2015**, *48*, 2213–2223. [CrossRef]
16. Li, J.; Kaunda, R.B.; Arora, S.; Hartlieb, P.; Nelson, P.P. Fully-coupled simulations of thermally-induced cracking in pegmatite due to microwave irradiation. *J. Rock Mech. Geotech. Eng.* **2019**, *11*, 242–250. [CrossRef]
17. Ma, Z.; Zheng, Y.; Gao, M.; Li, J. Assessing the Size Effect on Microwave Fracturing of Diorite Using a Dielectric-Loaded Converging Waveguide Antenna. *Rock Mech. Rock Eng.* **2023**, *56*, 5677–5691. [CrossRef]
18. Ferrari-John, R.S.; Batchelor, A.R.; Katrib, J.; Dodds, C.; Kingman, S.W. Understanding selectivity in radio frequency and microwave sorting of porphyry copper ores. *Int. J. Miner. Process.* **2016**, *155*, 64–73. [CrossRef]
19. Hassani, F.; Nekoovaght, P.M.; Gharib, N. The influence of microwave irradiation on rocks for microwaveassisted underground excavation. *J. Rock Mech. Geotech. Eng.* **2016**, *8*, 1–15. [CrossRef]
20. Meisels, R.; Toifl, M.; Hartlieb, P.; Kuchar, F.; Antretter, T. Microwave propagation and absorption and its thermo-mechanical consequences in heterogeneous rocks. *Int. J. Miner. Process.* **2015**, *135*, 40–51. [CrossRef]
21. Toifl, M.; Hartlieb, P.; Meisels, R.; Antretter, T.; Kuchar, F. Numerical study of the influence of irradiation parameters on the microwave-induced stresses in granite. *Miner. Eng.* **2017**, *103*, 78–92. [CrossRef]
22. Li, X.; Wang, S.; Xia, K.; Tong, T. Dynamic Tensile Response of a Microwave Damaged Granitic Rock. *ExM* **2021**, *61*, 461–468. [CrossRef]
23. Wang, S.; Xu, Y.; Xia, K.; Tong, T. Dynamic fragmentation of microwave irradiated rock. *J. Rock Mech. Geotech. Eng.* **2021**, *13*, 300–310. [CrossRef]
24. Liu, S.; Xu, J. Study on dynamic characteristics of marble under impact loading and high temperature. *Int. J. Rock Mech. Min. Sci.* **2013**, *62*, 51–58. [CrossRef]
25. Yao, W.; Xu, Y.; Wang, W.; Kanopolous, P. Dependence of Dynamic Tensile Strength of Longyou Sandstone on Heat-Treatment Temperature and Loading Rate. *Rock Mech. Rock Eng.* **2016**, *49*, 3899–3915. [CrossRef]
26. Zhao, Y.; Wan, Z.; Feng, Z.; Yang, D.; Zhang, Y.; Qu, F. Triaxial compression system for rock testing under high temperature and high pressure. *Int. J. Rock Mech. Min. Sci.* **2012**, *52*, 132–138. [CrossRef]
27. Huang, S.; Xia, K. Effect of heat-treatment on the dynamic compressive strength of Longyou sandstone. *Eng. Geol.* **2015**, *191*, 1–7. [CrossRef]
28. Li, M.; Mao, X.; Cao, L.; Pu, H.; Mao, R.; Lu, A. Effects of Thermal Treatment on the Dynamic Mechanical Properties of Coal Measures Sandstone. *Rock Mech. Rock Eng.* **2016**, *49*, 3525–3539. [CrossRef]
29. Xu, Y.; Yao, W.; Wang, S.; Xia, K. Investigation of the Heat-Treatment Effect on Rock Fragmentation Characteristics Using the Dynamic Ball Compression Test. *Rock Mech. Rock Eng.* **2020**, *53*, 2095–2108. [CrossRef]
30. Yao, W.; Xia, K.; Liu, H.-W. Influence of heating on the dynamic tensile strength of two mortars: Experiments and models. *Int. J. Impact Eng.* **2018**, *122*, 407–418. [CrossRef]
31. Wong, L.N.Y.; Li, Z.; Kang, H.M.; Teh, C.I. Dynamic Loading of Carrara Marble in a Heated State. *Rock Mech. Rock Eng.* **2017**, *50*, 1487–1505. [CrossRef]

32. Hartlieb, P.; Grafe, B.; Shepel, T.; Malovyk, A.; Akbari, B. Experimental study on artificially induced crack patterns and their consequences on mechanical excavation processes. *Int. J. Rock Mech. Min. Sci.* **2017**, *100*, 160–169. [CrossRef]
33. Nicco, M.; Holley, E.A.; Hartlieb, P.; Pfaff, K. Textural and Mineralogical Controls on Microwave-Induced Cracking in Granites. *Rock Mech. Rock Eng.* **2020**, *53*, 4745–4765. [CrossRef]
34. Yang, S.-Q.; Ranjith, P.G.; Jing, H.-W.; Tian, W.-L.; Ju, Y. An experimental investigation on thermal damage and failure mechanical behavior of granite after exposure to different high temperature treatments. *Geothermics* **2017**, *65*, 180–197. [CrossRef]
35. Yao, W.; Liu, H.-W.; Xu, Y.; Xia, K.; Zhu, J. Thermal degradation of dynamic compressive strength for two mortars. *Constr. Build. Mater.* **2017**, *136*, 139–152. [CrossRef]
36. Saroglou, C.; Kallimogiannis, V. Fracturing process and effect of fracturing degree on wave velocity of a crystalline rock. *J. Rock Mech. Geotech. Eng.* **2017**, *9*, 797–806. [CrossRef]
37. Zhou, Y.X.; Xia, K.; Li, X.B.; Li, H.B.; Ma, G.W.; Zhao, J.; Zhou, Z.L.; Dai, F. Suggested methods for determining the dynamic strength parameters and mode-I fracture toughness of rock materials. *Int. J. Rock Mech. Min. Sci.* **2012**, *49*, 105–112. [CrossRef]
38. Dai, F.; Huang, S.; Xia, K.; Tan, Z. Some Fundamental Issues in Dynamic Compression and Tension Tests of Rocks Using Split Hopkinson Pressure Bar. *Rock Mech. Rock Eng.* **2010**, *43*, 657–666. [CrossRef]
39. Fuenkajorn, K.; Klanphumeesri, S. Laboratory Determination of Direct Tensile Strength and Deformability of Intact Rocks. *Geotech. Test. J.* **2011**, *34*, 97–102. [CrossRef]
40. Li, D.; Wong, L.N.Y. The Brazilian Disc Test for Rock Mechanics Applications: Review and New Insights. *Rock Mech. Rock Eng.* **2013**, *46*, 269–287. [CrossRef]
41. Xia, K.; Yao, W.; Wu, B. Dynamic rock tensile strengths of Laurentian granite: Experimental observation and micromechanical model. *J. Rock Mech. Geotech. Eng.* **2017**, *9*, 116–124. [CrossRef]
42. Yin, T.; Wu, B.; Wang, C.; Wu, Y. Determination of Dynamic Tensile Strength of Microwave-Induced Basalt Using Brazilian Test. *Rock Mech. Rock Eng.* **2022**, *55*, 1429–1443. [CrossRef]
43. Xia, K.; Yu, Y.; Wu, B.; Yao, W. Correction of dynamic Brazilian disc tensile strength of rocks under preloading conditions considering the overload phenomenon and invoking the Griffith criterion. *J. Rock Mech. Geotech. Eng.* **2023**, *15*, 1986–1996. [CrossRef]
44. Xia, K.; Yu, Y.; Wang, S.; Wu, B.; Xu, Y.; Cai, Y. On the overload phenomenon in dynamic Brazilian disk experiments of rocks. *Explos. Shock Waves* **2021**, *41*, 041403.
45. Mishra, S.; Khetwal, A.; Chakraborty, T. Dynamic Characterisation of Gneiss. *Rock Mech. Rock Eng.* **2019**, *52*, 61–81. [CrossRef]
46. Zhu, Z.; Tian, H.; Mei, G.; Jiang, G.; Dou, B.; Xiao, P. Experimental investigation on mechanical behaviors of Nanan granite after thermal treatment under conventional triaxial compression. *Environ. Earth Sci.* **2021**, *80*, 46. [CrossRef]